Early sedimentation and crossover kinetics in an off-critical phase-separating liquid mixture

Jean Colombani, Jacques Bert

Early sedimentation and crossover kinetics in an off-critical phase-separating liquid mixture

J. Colombani* and J. Bert
Laboratoire Physique de la Matière Condensée et Nanostructures (UMR CNRS 5586), Université Claude Bernard Lyon 1, 6, rue Ampère, F-69622 Villeurbanne cedex, France

Early sedimentation in a liquid mixture off-critically quenched in its miscibility gap was investigated with a light attenuation technique. The time evolution of the droplets distribution is characteristic of an emulsion coalescing by gravitational collisions. This sedimentation behaviour has given access to the phase-separating kinetics and a crossover on the way toward equilibrium was observed, which separates free growth from conserved order-parameter coarsening with a crossover time fitting well to theoretical predictions.

PACS numbers: 64.75.+g, 64.60.My, 82.70.Kj, 47.20.Bp

I. INTRODUCTION

The study of liquid-liquid phase separation constitutes a unique opportunity of observing the decay modes to equilibrium of a system abruptly brought into a metastable or nonequilibrium state. One benefits here from the universal behaviour of the dynamical properties in the vicinity of a consolute critical point.

The leading quantity is the supersaturation Φ, corresponding to the equilibrium volume fraction of the minority phase. For values of Φ from $\frac{1}{2}$ to 0 —or equivalently from deep to shallow quenches in the miscibility gap— the following stages can be encountered :

- For critical, i.e., quasisymmetric, quenches ($\Phi \simeq \frac{1}{2}$), the phase-separating mechanism is spinodal decomposition and has been abundantly investigated. Incipient domains from both phases grow from the most unstable wavelength of the concentration fluctuations ξ^- [1]. Afterwards they coarsen by brownian collision-induced coalescence and the time evolution of their mean size scales as $t^{\frac{1}{3}}$ [2]. When they constitute a bicontinuous percolating medium, coarsening continues through surface-tension driven mechanisms (Rayleigh-like instability [3], coalescence-induced coalescence [4]) which induce a coarsening law linear with time [2].

- For off-critical, i.e., nonsymmetric, quenches, the phase-separating regime is nucleation and growth, where the nucleation has recently been stated as always being heterogeneous. This statement has been inferred from the monodispersity [5] and the undercriticality [6] of the nucleated droplets size. Growth proceeds through the diffusion of one of the components from the supersaturated background to a fixed number of growing nuclei ('free growth') with a $t^{\frac{1}{2}}$ law [7]. After an intermediate regime where the volume fraction of minority phase reaches its equilibrium value Φ, two competing mechanisms are expected. First when the solute-depleted layers around the growing droplets begin to interact, the coarsening mechanism may become Ostwald ripening, i.e., evaporation-condensation (undercritical nuclei dissipate into critical ones), obeying the $t^{\frac{1}{3}}$ Lifschitz-Slyozov (LS) law [8]. Parallely, as for the spinodal decomposition, when interfaces become sharp, coalescence may proceed through brownian diffusion (BD) induced collisions of droplets, which implies also a $t^{\frac{1}{3}}$ law, with a different prefactor from LS's one [3]. The latter process should prevail at high Φ values and late times.

The volume fraction of minority phase Φ_T separating these two scenarii has been subject to much discussion but the latest reliable value should be $\phi_T \simeq 30\%$[9]. Few results are available where Φ is systematically scanned between 0 and ϕ_T [9, 10]. Hence some points remain questionable among which the precise domain of existence of BD and LS coarsenings and the time of crossover between the free diffusion ($t^{\frac{1}{2}}$) and conserved order-parameter ($t^{\frac{1}{3}}$) regimes.

Whatever the regime, when the droplet size reaches a threshold value, gravity begins to prevail and sedimentation occurs. In the critical regime, two contributions to the study of sedimentation have to be mentionned. The first one identifies the successive stages during the prevailing of gravity [11]: Macroscopic convection, sedimentation of droplets leading to a t^3 growth law, appearing of a meniscus sharing the mixture in two macroscopic phases, residual sedimentation. The second one identifies the growth law during this residual sedimentation stage as $t^{0.27}$, as a consequence of coalescence by both sedimentation and brownian diffusion [12]. Besides, sedimentation in the off-critical regime has never been systematically investigated and it is our aim to explore it.

Unexpectedly, this sedimentation study gives the opportunity to probe early times of the separation dynamics, delicate to access with light scattering methods for instance [5]. Thereby we present here experimental evidence of a crossover on the way toward equilibrium of a

*Electronic address: Jean.Colombani@lpmcn.univ-lyon1.fr

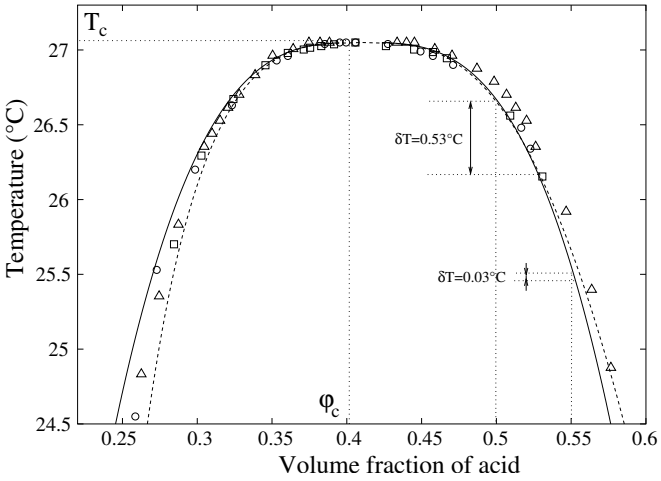

FIG. 1: Phase diagram (ϕ_{acid}, T) of the isobutyric acid-water mixture from Woermann *et al.* [13] (◯), Chu *et al.* [14] (□), Zhuang *et al.* [15] (△), Krall *et al.* [16] (dashed line) and Andrew *et al.* [17] (solid line). The critical temperatures have been matched to ours : T_c=27.05°C. Our shallowest and deepest quenches are also represented.

phase-separating mixture.

II. EXPERIMENTS

For this purpose, we have chosen the water-isobutyric acid mixture, taking advantage from its room-temperature miscibility gap and from the complete knowledge of its physicochemical properties.

Numerous experimental determinations of the phase diagram of this system may be found in the literature. To get a clear view of the experimental uncertainty (mentionned by Baumberger *et al.* [18]) on the coexistence curve, which is of former importance for the computation of the volume fraction of the growing phase Φ, we gathered the most representative experimental phase diagrams on a single volume fraction-temperature plot (cf. Fig. 1). The new processing of the values of Hamano *et al.* [19] by Krall *et al.* [16] and the more recent interpretation of Greer's density measurements [20] by Andrew *et al.* [17] have been chosen rather than the original corresponding works. The acid mass fraction values c_{acid} of Krall *et al.* [16], Woermann *et al.* [13], Zhuang *et al.* [15] and Chu *et al.* [14] have been turned into volume fraction values ϕ_{acid} through $\phi_{acid} = (\rho_{phase}/\rho_{acid})c_{acid}$, the densities ρ of the two phases and of isobutyric acid being taken from [20]. The critical temperature T_c shows a dispersion of more than one degree among the experiments, most certainly due to ionic impurities, which is of little consequence on the critical behaviour [20, 21]. So all curves have been adjusted to our experimental value $T_c = 27.05°C$. The data of Andrew *et al.* are quite recent and situated in the mean range of the other results [17]. Accordingly their expression for the miscibility gap

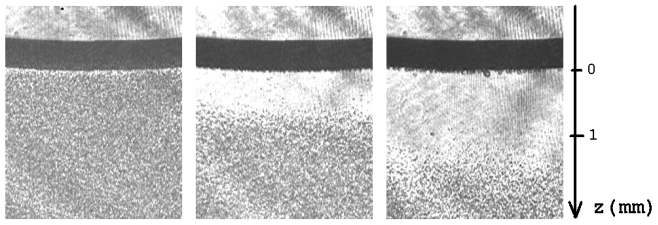

FIG. 2: Photographs of the sedimenting droplets in a mixture with ϕ_{acid}=54% for δT=0.13 K, 3.5, 23.5 and 43.5 min. after the quench.

$\Delta\phi_{acid} = \Delta\phi_0\epsilon^\beta$ with $\Delta\phi_{acid} = \phi_{acid} - \phi_c$, $\phi_c = 0.4028$, $\Delta\phi_0 = 1.565$, $\beta = 0.326$ and $\epsilon = (T_c - T)/T_c$ the reduced temperature, has been chosen for our computation of Φ.

For the correlation length of the concentration fluctuations along the binodal line, the expression $\xi^- = \xi_0\epsilon^{-\nu_\xi}$ with $\xi_0 = 1.8\mathring{A}$ and $\nu_\xi = 0.63$ has been chosen [16]. The viscosities are $\eta = (\eta^B + A'\epsilon^{\frac{1}{3}})\epsilon^{-0.04}$ for the acid-rich phase and $\eta' = (\eta^B - A'\epsilon^{\frac{1}{3}})\epsilon^{-0.04}$ for the water-rich phase, with $\eta^B = 1.89$ mPl and $A' = 2.60$ mPl [16]. The diffusion coefficient of the mixture along the acid-rich branch of the coexistence curve is deduced from the above quantities thanks to a Stokes-Einstein relation: $D^- = k_BT/(6\pi\eta\xi^-)$.

To perform the quenches, an optical fused quartz cell containing the mixture is inserted inside a hollow copper block where a thermostat ensures a water circulation, providing a temperature stabilization of the system within 0.01 K. The cell (optical pathlength 0.1 cm, 1 cm wide and 3 cm high) is illuminated by a laser beam and is observed by means of a Charge-Coupled Device camera. For each studied concentration, the temperature of the coexistence curve has been visually determined (cloud point method) by a slow decrease of the temperature from the one-phase mixture (0.01 K temperature steps, each followed by a 20 minutes stabilization).

Before each run, an energetic stirring is performed followed by a 12 hours annealing in the one-phase region 0.05 K above the coexistence curve. Then, the mixture is rapidly quenched through the binodal line (δT =0.03 to 0.53 K below it) and this incursion in the miscibility gap leads to the phase separation (cf. Fig. 2). In each case, the volume fraction of acid ϕ_{acid} (50 to 55%) and the reduced temperature $\epsilon_f = (T_c - T_f)/T_c$ (2.3 to 6.4×10^{-3} with T_f the absolute final temperature) are chosen in order to induce a volume fraction Φ of the growing phase between 0.3 and 10.5%. The water-rich phase (density $\rho' \simeq 998$ kg m^{-3}) has been chosen as the nucleating and sedimenting phase to prevent wetting effects. Indeed the isobutyric acid-rich phase (density $\rho \simeq 988$ kg m^{-3}) is known to preferentially wet the cell walls [17].

The evolution of the transmitted intensity along the vertical axis of the cell $I(z)$ is extracted from the video output —kept in its linear response domain— via an image processing software (cf. Fig. 2) An averaging of $I(z)$ along an horizontal segment in the middle of the cell is

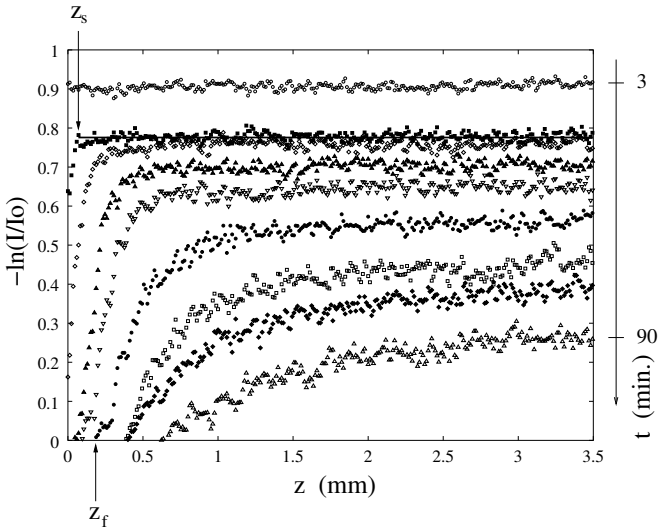

FIG. 3: Logarithm of the light attenuation $-ln(I/I_0)$ across the cell as a function of the vertical position z and elapsed time t for a volume fraction of acid $\phi_{acid} = 54\%$ and a quench depth δT =0.37 K.

carried out for each value of z to gain noise reduction. Then the light attenuation $I(z)/I_0$ is computed for several times during the phase separation. I_0 stands for the unscattered light intensity refracted by the homogeneous (droplet-free) mixture. This light attenuation is mainly due to scattering. The refraction indices of the two phases are very similar ($\Delta n \sim 10^{-2}$ in our ϵ range [17]), which is likely to induce a low multiscattering. So in our Φ range and assuming a small polydispersity, the light attenuation $I(z)/I_0$ is linked at a first order to the concentration of droplets $n(z)$ through the Lambert-Beer law $n(z) \sim -ln(I(z)/I_0)$. Therefore the evolution of the $-ln(I(z)/I_0)$ curves with time reports on the change of spatial distribution of droplets during sedimentation as displayed in Fig. 3.

The droplets being larger than the laser wavelength λ =0.532 μm (see below), the attenuation should also be inversely proportional to their squared radius, which could have a slight influence on $-ln(I/I_0)$. Therefore this expression constitutes a qualitative evaluation of n but our analysis does not require a more precise determination, dealing only with abrupt slope changes in the behaviour of n.

The time origin has been chosen as the cloud appearance time and the space origin as the lower limit of the liquid-air meniscus (cf. Fig. 2).

Right after the quench, the cell becomes uniformly filled with erratically moving droplets forming an opalescent mist (horizontal upper line in Fig. 3). Then in the vicinity of the meniscus the droplet concentration progressively decreases down to a zero value owing to an overall vertical motion of the droplets only visible at the top (clarification zone, droplet-free) and the bottom (sedimentation layer, not shown in Fig. 2 and 3) of the vessel. Afterwards, the initial point z_f of the curves moves down and the value of the plateau sinks. The first feature reflects a growth of the clarification zone and the second one owes to the decrease of the bulk droplet concentration due to coalescence yielded by brownian and/or gravitational collisions.

III. COARSENING MECHANISM DURING SEDIMENTATION

In order to highlight the respective role of the brownian and gravitational processes, the knowledge of the Péclet number $Pe = vR/D$ is needed (v mean sedimentation velocity, R radius and D diffusion coefficient of the droplets). Indeed this number compares the mean sedimentation velocity v to a brownian velocity D/R.

With this purpose, we turn to the clarification zone behavior. Its growth can be followed in Fig. 3 through the increase with time of the interceipt z_f with time of the light attenuation curve with the abscissa axis. In other words, z_f corresponds to the upper limit of the sedimentation front. At this point, the droplets are very scarce so they can be considered as evolving in a quasi-infinitely dilute regime. Therefore the sedimentation-induced convective part of their motion is insignificant [22] and their velocity v_f corresponds to the stationary velocity of isolated droplets of radius R_f, given by the Hadamard formula [23]:

$$v_f = \frac{2(\eta' + \eta)(\rho' - \rho)R_f^2 g}{3(3\eta' + 2\eta)\eta} \qquad (1)$$

with g the gravitational acceleration, η' and η respectively the viscosity of the water-rich drop and of the acid-rich surrounding fluid, ρ' and ρ their respective density. To assess the validity of this expression, two checkings have been carried out. This formula is valid provided that inertia effects are negligible. This requirement is guaranteed by a low Reynolds number $Re = R_f v_f \rho/\eta$, always smaller than 2.10^{-6} in our case. Secondly, even if long-range interdroplet hydrodynamic interactions induced an average settling velocity v_{av} lower than the Hadamard velocity v_f, the hindered settling function $f(c) = v_{av}/v_f$ would take values between $\frac{1}{2}$ and 1 for Φ ranging from 1 to 10% [22]. So these interactions would not yield a noticeable change of the value of the settling velocity.

As v_f is given by the slope of the $z_f(t)$ line (cf. Fig. 4), the droplet radius R_f at the appearance of the clarification zone can be computed from Eq. 1. R_f ranges between 3.3 and 8.9 μm. Knowing that the diffusivity of spherical droplets immersed in a liquid of viscosity η is $D_f = k_B T/(5\pi\eta R_f)$ [29], their Péclet number $Pe_f = v_f R_f/D_f$ can be computed:

$$Pe_f = \frac{15\pi\eta^2(3\eta' + 2\eta)v_f^2}{2k_B T(\eta' + \eta)(\rho' - \rho)g}. \qquad (2)$$

Pe_f is found to range between 8 (ϕ_{acid} = 50% and $\delta T = 0.53$°C) and 371 (ϕ_{acid} = 53% and $\delta T = 0.13$°C).

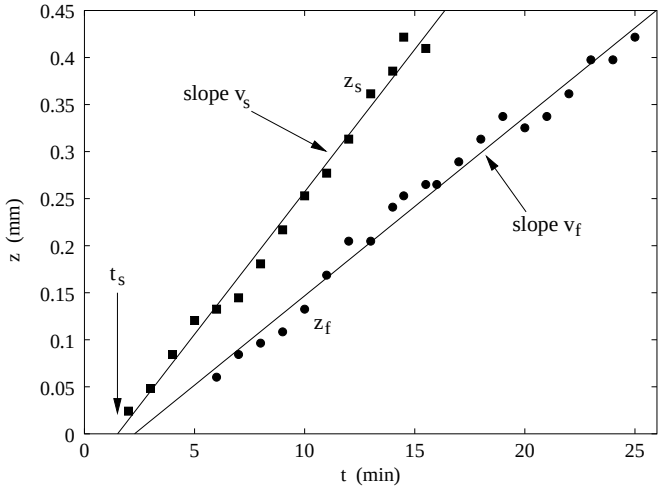

FIG. 4: Position of the beginning point z_f and of the start of the plateau z_s of the light attenuation curves as a function of time in the ($\phi_{acid} = 52\%, \delta T$ =0.12 K) case. The lines are least-square fits of the values. The t_s time is also shown.

Recalling that these droplets experience almost no coalescence owing to their dilute environment, their growth is the slowest of the vessel, their radius is the smallest, and their velocity is minimal among all droplets, so we can argue that $Pe \gg 1$ in the bulk sedimenting liquid. Therefore gravitation-induced hydrodynamic interactions should prevail over brownian diffusion as the coalescence mechanism.

To confirm this statement, we consider theoretical studies on coalescence of non-brownian sedimenting polydisperse droplets immersed in an immiscible fluid [24]. The evolution of the volume fraction of droplets with position in the vessel at different times (Fig. 7 of Ref. [24]) shows a strong closeness with our light attenuation curves of Fig. 3. Therefore the droplet density in our sedimenting mixture displays the same evolution as predicted for non-brownian droplets and, at variance with some predictions [12, 18], the driving force of coalescence is likely to consist only of gravitational collisions.

IV. PHASE SEPARATION DYNAMICS

What can we learn now about the drops growth law during this stage of phase separation? To address this point, we focus on the early appearance of sedimentation. When growing droplets experience a gravitational force overwhelming brownian diffusion, the symmetry of their displacement is broken and they exhibit an average descending motion. This incipient settling motion can be traced in Fig. 3 through the displacement with time of the beginning z_s of the curves plateau. In other words, we follow with z_s the initial mean trajectory of the droplets settling from the meniscus. We concentrate on early times, where the interceipt of the rising curve and the plateau is unambiguous. If the Péclet number Pe_s, mean sedimentation velocity v_s, and diffusivity D_s of these settling droplets are known independantly, their radius can be computed, considering the definition of Pe_s, via $R_s = \sqrt{Pe_s D_s / v_s}$. Using the above-mentionned Stokes-Einstein expression for D_s, one gets $R_s = \sqrt{Pe_s k_B T/(5\pi\eta v_s)}$.

The value of η is given above and v_s is accessible through the slope of the $z_s(t)$ line (cf. Fig. 4). So at this point, we need a determination of the only missing value, Pe_s, to be able to calculate R_s at least at one particular time of the coarsening.

The sedimentation regime is entered when the Péclet number sufficiently exceeds unity. We will tentatively consider that this is the case when the sedimentation velocity becomes one order of magnitude larger than the diffusive velocity. The time t_s of this start of sedimentation is measured in extrapolating the $z_s(t)$ curve to zero. $z_s(t)$ has been seen to remain linear at early times, which enables a well-defined extrapolation of t_s (cf. Fig. 4). So at t_s we assume that $Pe_s = 10$ and R_s can be computed with the above-mentioned formula. As expected for droplets at the non sedimenting-sedimenting transition, R_s ranges between 1.0 and 3.2 μm for our quenches.

Therefore we use our knowledge of the sedimentation behaviour as a probe to determine the droplet radius R_s just when sedimentation sets in. Accordingly, the R_s values of the different quenches are characteristic of the early coarsening mechanisms preceding sedimentation (free growth, BD, LS) and not related to the settling behaviour itself.

Concerning the choice of Pe_s, Wang and Davis have performed computations in an immiscible mixture experiencing simultaneous brownian and gravitational collisions [25]. Using their predictions, we have computed the mean radius R_s of the coalescing droplets after a time estimated as t_s in the most unfavourable case of viscosity, dispersity and settling velocity. We find that $R_s \simeq 1.5\ R_0$ (R_0 initial radius) for an initial Péclet number $Pe_s = 1$ and $R_s \simeq 2.4\ R_0$ for $Pe_s = 10$. Therefore we can conclude that 1) whatever the choice of Pe_s, gravity has not significantly modified the coarsening dynamics after an elapsed time t_s and 2) this minor influence on R_s, if any, is comparable for Pe_s ranging from 1 to 10. Furthermore $R_s \sim \sqrt{Pe_s}$ which induces a weak influence of the choice of Pe_s, between 1 and 10, on the computation of R_s.

To allow comparison between the dynamics of all experiments, we put the time and radius values in a dimensionless form : $\tau = t/t_c$ and $\rho = R/R_c$. The renormalization quantities are the radius of an initial critical nucleus $R_c = \alpha/\Phi$ and the relaxation time of this nucleus $t_c = D^- \alpha^2/\Phi^3$, with α a capillary length estimated as $\alpha = \xi^-/3$ [7].

We benefit now from one point (τ_s, ρ_s) for each experiment, covering five decades of reduced time. Fig. 5 displays the evolution of ρ_s as a function of τ_s. We first ascertain that all experiments merge onto a single curve, whatever the initial supersaturation. The second striking feature lies in the presence of a crossover be-

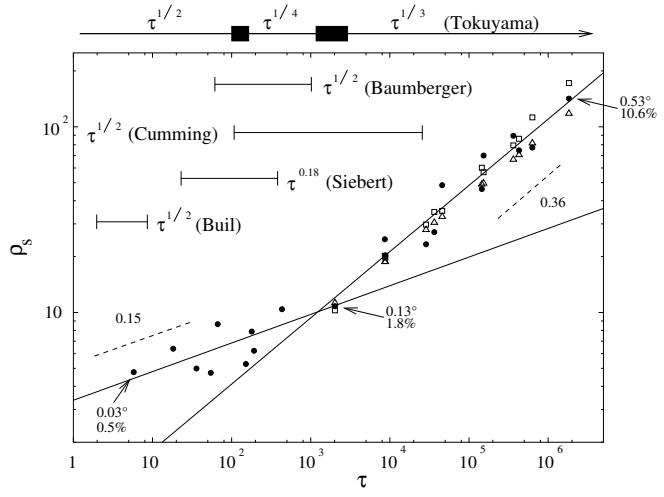

FIG. 5: Evolution with reduced time τ of the reduced droplet size ρ_s at the end of the non-sedimenting regime (black dots). The open triangles and squares are respectively the theoretical values of ρ_s for an Ostwald ripening and a brownian diffusion-coalescence growth. It should be noticed that each point corresponds to one experiment. Ranges of growth exponents available in the literature for $\Phi < 10\%$ have also been added (references given in the text). The quench depth δT and the volume fraction of the growing phase Φ have been mentionned for some representative points.

tween two coarsening stages. The first behaviour can tentatively be fitted by a power law of exponent $\simeq 0.15$. Such a slow radius evolution is expected at the end of the free growth regime and reflects the overlapping of the solute-depleted shells around the nuclei [26]. The second behaviour displays a growth exponent $0.36 \simeq \frac{1}{3}$ which is the well-known exponent of interface-reduction coarsenings (LS and BD). To our knowledge this constitutes the first experimental observation of the crossover between free growth and constant volume-fraction coarsening in a liquid system. This crossover takes place at $\tau_{CO} \simeq 1 \times 10^3$.

The experimental and theoretical growth laws available for $\Phi < 10\%$ in the literature have also been added in Fig. 5. Surprisingly, no other measurements exist in the $t^{\frac{1}{3}}$ range for $\Phi < 10\%$ except those of Wong & Knobler which seem to display a progressive change of slope and are therefore delicate to deal with [2] and those of White & Wiltzius, the dimensionless parameters of which are not available [27]. Concerning the end of free diffusion, our growth exponent is equivalent to Siebert & Knobler's one (0.18) [28] and is compatible with the theoretical prediction of Tokuyama & Enomoto ($\frac{1}{4}$) [26]. The validity domain of this intermediate stage is also compatible with the $t^{\frac{1}{2}}$ range of Buil *et al.* [6] but is not consistent with those of Baumberger *et al.* [18] and Cumming *et al.* [5]. The latter dealt with polymer blends and this could account for the dynamics discrepancy or at least for the difficulty of computing equivalent dimensionless quantities in simple (acid/water) and complex (polymer blends) fluids. The inconsistency with the former remains unexplained. The crossover time compares well with Tokuyama & Enomoto's theoretical value $1.1 \times 10^3 < \tau_{CO}^{theo} < 2.8 \times 10^3$, the lower value computed at $\Phi = 1\%$ and the upper one at $\Phi = 10\%$ [26].

As the exact mechanism of the late decompositional stage still remains debatable [27], we have drawn in Fig. 5 the theoretical values of $\rho_s(\tau)$ predicted by the Lifschitz-Slyozov and brownian diffusion coarsening laws, computed without adjustable parameters. Written in reduced units, the expressions are $\rho_s = [1 + (4/9)f(\Phi)\tau]^{\frac{1}{3}}$ ($f(\Phi)$ being a numerically estimated function) for evaporation-condensation [8] and $\rho_s = [144\Phi/(\ln(0.55R_s/\delta))]^{\frac{1}{3}}$ (with $\delta \simeq \xi^-$) for brownian diffusion coalescence [3]. Unfortunately, though experimental and theoretical values superimpose [30], the dispersion of our values is too large to discriminate between the LS and BD laws, and their closeness banish any hope to do so from $\rho(\tau)$ curves.

V. CONCLUSION

We have determined the leading coarsening mechanism (gravitational collisions) during the sedimentation regime in a homogeneous mixture plunged in a metastable state. Besides, thanks to the superposition of numerous sedimentation experiments in such systems, the universal crossover time between free growth and ripening by diffusion of a conserved order-parameter has been measured and agrees with theoretical predictions. Unfortunately the nature of the second mechanism has not been settled and the existence range of Ostwald ripening and brownian coalescence coarsening remains to be established. Finally, an experimental access to the complete scenario of the off-critical coarsening from the $t^{\frac{1}{2}}$ to the $t^{\frac{1}{3}}$ law would bring a comprehensive view of the phase-separation process and a complete verification of the nucleation and growth theory.

Acknowledgments

We acknowledge CNES (french space agency) for financial support, Bénédicte Hervé, Laurence Heinrich and Richard Cohen for experimental help, and Jean-Pierre Delville, Régis Wunenburger, Christophe Ybert and Elisabeth Charlaix for fruitful discussions.

[1] J. Cahn, Trans. Metall. Soc. AIME **242**, 166 (1968).

[2] N. Wong and C. Knobler, Phys. Rev. A **24**, 3205 (1981).

[3] E. Siggia, Phys. Rev. A **20**, 595 (1979).
[4] V. Nikolayev, D. Beysens, and P. Guénoun, Phys. Rev. Lett. **76**, 3144 (1996).
[5] A. Cumming, P. Wiltzius, F. Bates, and J. Rosedale, Phys. Rev. A **45**, 885 (1992).
[6] S. Buil, J. Delville, and A. Ducasse, Phys. Rev. Lett. **82**, 1895 (1999).
[7] J. Langer and A. Schwartz, Phys. Rev. A **21**, 948 (1980).
[8] N. Akaiwa and P. Voorhees, Phys. Rev. E **49**, 3860 (1994).
[9] F. Perrot, D. Beysens, Y. Garrabos, T. Fröhlich, P. Guenoun, M. Bonetti, and P. Bravais, Phys. Rev. E **59**, 3079 (1999).
[10] I. Hopkinson and M. Myatt, Macromolecules **35**, 5153 (2002).
[11] C. Chan and W. Goldburg, Phys. Rev. Lett. **58**, 674 (1987).
[12] F. Cau and S. Lacelle, Phys. Rev. E **47**, 1429 (1993).
[13] D. Woermann and W. Sarholz, Ber. Bunsenges. Phys. Chem. **69**, 319 (1965).
[14] B. Chu, F. Schoenes, and W. Kao, J. Am. Chem. Soc. **90**, 3042 (1968).
[15] Z. Zhuang, A. Casielles, and D. Cannell, Phys. Rev. Lett. **77**, 2969 (1996).
[16] A. Krall, J. Sengers, and K. Hamano, Phys. Rev. E **48**, 357 (1993).
[17] W. Andrew, T. Khoo, and D. Jacobs, J. Chem. Phys. **85**, 3985 (1986).
[18] T. Baumberger, F. Perrot, and D. Beysens, Phys. Rev. A **46**, 7636 (1992).
[19] K. Hamano, S. Teshigawara, T. Koyama, and N. Kuwahara, Phys. Rev. A **33**, 485 (1986).
[20] S. Greer, Phys. Rev. A **14**, 1770 (1976).
[21] R. Cohn and D. Jacobs, J. Chem. Phys. **80**, 856 (1984).
[22] R. Davis and A. Acrivos, Ann. Rev. Fluid Mech. **17**, 91 (1985).
[23] J. Hadamard, C.R. Acad. Sci. Paris **152**, 1735 (1911).
[24] H. Wang and R. Davis, J. Fluid Mech. **295**, 247 (1995).
[25] H. Wang and R. Davis, J. Colloid Interface Sci. **178**, 47 (1996).
[26] M. Tokuyama and Y. Enomoto, Phys. Rev. Lett. **69**, 312 (1992).
[27] W. White and P. Wiltzius, Phys. Rev. Lett. **75**, 3012 (1995).
[28] E. Siebert and C. Knobler, Phys. Rev. Lett. **54**, 819 (1985).
[29] This expression is obtained in writing, in the Stokes-Einstein expression of the diffusivity of one droplet $D = \frac{k_B T}{\mu}$, the mobility μ as v_f/F_g with v_f the Hadamard sedimentation velocity of Eq. 1 taken with $\eta = \eta'$ and $F_g = (\rho' - \rho) g \frac{4}{3} \pi R_f^3$ the gravitational force exerting on the droplet.
[30] This superimposition justifies *a posteriori* our $Pe_s = 10$ choice for the computation of ρ_s. Nevertheless a change in Pe_s would have only implied a vertical translation of the values but would have had no influence on the kinetics and crossover time.